Vibrational Spectrum Associated with the Reduction of Tyrosyl Radical D• in Photosystem II: A Comparative Biochemical and Kinetic Study†

Sunyoung Kim and Bridgette A. Barry*

University of Minnesota, Department of Biochemistry, Molecular Biology, and Biophysics, St. Paul, Minnesota 55108-1022

Received June 3, 1998; Revised Manuscript Received July 27, 1998

ABSTRACT: Photosystem II (PSII) contains a redox-active tyrosine, D. Difference FT-IR spectroscopy can be used to obtain structural information about this species, which is a neutral radical, D•, in the photooxidized form. Previously, we have used isotopic labeling, site-directed mutagenesis, and kinetics to assign a vibrational line at 1477 cm^{-1} to D•; these studies were performed on highly resolved PSII preparations at pH 7.5 {Kim et al. (1998) *Biochim. Biophys. Acta 1364*, 337−360; publisher's correction, *Biochim. Biophys. Acta 1366*, 330−354}. Here, we use kinetics to assign vibrational features to tyrosyl radical, D•, in PSII membranes. EPR and fluorescence controls identify a time regime in which D• decay occurs independently of redox changes involving the PSII quinone acceptors. Difference FT-IR spectra, acquired over this time regime, exhibit decreases in the amplitude of a 1477 cm^{-1} line; quantitative comparison with EPR transients supports the assignment to D•. Conditions, requiring the use of phosphate/formate, have been described for observation of a dissimilar FT-IR spectrum, which has been assigned to tyrosyl radical D•; this spectrum lacks a 1477 cm^{-1} line {Hienerwadel et al. (1997) *Biochemistry 36*, 14712−14723}. Under these conditions, we have observed (1) an acceleration in the rate of D• decay and a decrease in D• yield attributable to the presence of formate, (2) a proportional decrease in the amplitude of FT-IR spectra acquired over the time regime in which D• decays, (3) frequency shifts in the D• − D FT-IR spectrum, (4) large-scale structural changes, as assessed by the amide I line shape, and (5) contributions to the FT-IR spectrum from the phosphate/formate buffer in the absence of PSII. We conclude that changes in the FT-IR spectrum, observed in the presence of phosphate/formate, are caused by alterations in the environment of D• and by direct phosphate/formate contributions to the spectrum.

Photosystem II (PSII),[1] which is a multisubunit protein complex within the thylakoid membrane, performs both charge separation and water oxidation upon photoexcitation in plants, algae, and cyanobacteria. The majority of the cofactors involved in charge separation are bound to two polypeptides, termed D1 and D2; the known prosthetic groups involved in electron transfer are the specialized chlorophyll P_{680}, pheophytin, and the quinones Q_A and Q_B. Upon light excitation, an electron is transferred in successive steps from P_{680} to the quinone moieties. The photooxidized P_{680}^+ is reduced by a redox-active tyrosine Z, which is tyrosine 161 in the D1 polypeptide. Tyrosyl Z• subsequently oxidizes the catalytic site, which contains four manganese atoms. The release of oxygen from water requires four sequential oxidation steps. The catalytic site cycles through five intermediate states, called the S_n states, where *n* refers to the number of oxidizing equivalents stored (reviewed in refs *1* and *2*).

In addition to tyrosine Z, there is another redox-active tyrosine, D, on the donor side of PSII (*3*); tyrosine D is residue 160 in the D2 polypeptide (*4*, *5*). Tyrosyl D• is stable in the dark for hours; the rate of tyrosyl D• decay increases at higher pH (*6*). Tyrosine D is oxidized by P_{680}^+ (*7*).

Difference (light-minus-dark) Fourier transform infrared (FT-IR) spectroscopy can be used to obtain information about structural changes that accompany light-induced processes in proteins (*8*). Difference FT-IR spectroscopy is still a relatively new technique in its application to PSII (see, for example, refs *9*−*13*). The use of difference techniques facilitates a detailed examination of the structure and/or dynamics of a protein. Another advantage of FT-IR spectroscopy is that time-resolved techniques can be used to track important structural changes, which occur along the enzymatic reaction pathway.

As a case in point, FT-IR spectroscopy has been used to obtain information about the redox-active tyrosines in PSII and about the interaction of each tyrosine with its environment (*11*, *14*−*18*). The vibrational spectrum associated with tyrosine D oxidation in highly resolved cyanobacterial and plant PSII preparations has been obtained; site-directed mutagenesis, isotopic labeling, and kinetic studies were used to assign the spectrum (*11*, *15*−*18*). The proton-accepting species for tyrosine D was observed and identified in the

† Supported by NIH GM 43273 (B.A.B.).

* Corresponding author: University of Minnesota, Department of Biochemistry, 1479 Gortner Avenue, St. Paul, MN 55108. Phone: 612-624-6732. Fax: 612-625-5780. E-mail: barry@biosci.cbs.umn.edu.

[1] Abbreviations: chl, chlorophyll; D, tyrosine 160 in the D2 polypeptide of photosystem II; DCBQ, 2,6-dichloro-*p*-benzoquinone; DCMU, 3-(3,4-dichlorophenyl)-1,1-dimethylurea; EPR, electron paramagnetic resonance spectroscopy; FT-IR, Fourier transform infrared spectroscopy; HEPES, *N*-(2-hydroxylethyl)piperzine-*N*′-(2-ethanesulfonic acid); MES, 2-(*N*-morpholino)ethanesulfonic acid; PSII, photosystem II; Tris, tris(hydroxylmethyl)aminomethane; Z, tyrosine 161 in the D1 polypeptide of photosystem II.

S0006-2960(98)01318-X CCC: $15.00
Published on Web 09/05/1998

difference FT-IR spectrum, D• − D; the identification of the proton acceptor was performed through the use of chemical complementation (*11*). The D• − D spectrum, obtained in these highly resolved cyanobacterial and plant preparations, exhibits an intense spectral feature at 1477 cm^{-1}. This vibrational feature has been assigned to the C−O vibration of tyrosyl radical, D• (*17*). On the other hand, under alternate conditions, a dissimilar spectrum has been assigned to tyrosine D (*10*, *19*). Observation of this spectrum is dependent on the presence of high concentrations of phosphate and formate (*19*), and this spectrum does not exhibit intensity at 1477 cm^{-1}. Here, we obtain difference FT-IR spectra under the conditions previously described (*19*). Our experiments provide an explanation for the spectral changes observed in the presence of phosphate and formate.

MATERIALS AND METHODS

Sample Preparation. Photosystem II membranes, containing 274 chl/reaction center (*20*), were purified from market spinach (*21*). The chlorophyll determination was performed in 80% acetone (*22*). Oxygen rates of isolated PSII membranes before manganese-depletion were between 1000 and 1100 μmol of O_2 (mg of chl)$^{-1}$ h^{-1}, in an assay buffer containing 0.4 M sucrose, 50 mM MES−NaOH (pH 6.0), 10 mM NaCl, 1 mM recrystallized DCBQ, and 1 mM potassium ferricyanide. PSII samples were manganese-depleted using 0.8 M Tris-HCl (pH 8.0) and 2 mM EDTA (*19*). The sample was split into two fractions. One fraction was washed in successive rounds of N_2-degassed 50 mM NaH_2PO_4/Na_2HPO_4 (pH 6.0), 100 mM sodium formate, 10 mM NaCl, and 15 mM $MgCl_2$ (*19*) and incubated for 1 h in the dark. The final pellet was resuspended in 50 mM NaH_2PO_4/Na_2HPO_4 (pH 6.0), 50 mM sodium formate, 10 mM NaCl, and 15 mM $MgCl_2$ (phosphate/formate buffer). The second fraction was resuspended in 5 mM HEPES−NaOH, pH 7.5 (HEPES buffer), after an identical number of wash steps. Final concentrations were 3.2−4.2 and 3.2−5.1 mg chl/mL for the HEPES and phosphate/formate PSII samples, respectively. Samples were frozen in liquid nitrogen and were stored at −80 °C until use.

To examine the effect of individual components of the phosphate/formate buffer, manganese-depleted PSII membranes were also washed and resuspended in buffers containing 5 mM or 50 mM MES−NaOH, pH 6.0. The incubation for 1 h was omitted for these samples. When present, the phosphate concentration was 50 mM NaH_2PO_4/Na_2HPO_4 and the formate concentration was 50 mM sodium formate. Fluorescence, EPR, and difference FT-IR measurements were performed on identical PSII samples. The above three spectroscopies were employed on multiple samples from different preparations of PSII membranes, to account for any variation in PSII samples.

EPR Measurements. EPR spectra, acquired at −9 °C, were obtained using a Bruker EMX 6/1 spectrometer equipped with a Bruker ST-TE cavity and a Wilmad variable temperature Dewar (*17*). The desired −9 °C cavity temperature was maintained using a stream of cold nitrogen through a dry ice ethanol bath. Samples were illuminated in the cavity using red- and heat-filtered light from a fiber-optic illuminator (Dolan Jenner, Woburn, MA). For examination of tyrosyl radicals in the above manganese-depleted spinach PSII preparations, 100 μL of sample, which was identical to the sample used for fluorescence and FT-IR measurements, was partially dehydrated on Mylar strips (*14*, *16*, *17*). Immediately prior to drying, 3 mM potassium ferricyanide/3 mM potassium ferrocyanide or 48 mM potassium ferricyanide (*10*, *19*) was added to the manganese-depleted PSII samples in HEPES or phosphate/formate buffers, respectively. The volumes of exogenous acceptors added were approximately equivalent. Spectra were corrected for differences in protein concentration and gain. Spin quantitation was performed by double integration of the spectrum as previously described (*23*).

Difference FT-IR Measurements. Infrared spectra were obtained at −9 °C, using a Magna 550 II spectrometer with KBr beam splitter and a MCT/A detector (Nicolet, Madison, WI) (*17*). Temperature maintenance at −9 °C and the automated illumination system, which was red- and heat-filtered, were previously described (*17*). Spectral conditions in these experiments were similar to those previously described (*17*, *18*).

In the data collection for difference FT-IR measurements, 48 scans, collected in 20 s, were coadded for each double-sided interferogram. Spectral conditions were as follows: resolution, 8 cm^{-1}; zero filling, one level; velocity, 2.5 cm/s; apodization function, Happ−Genzel; and temperature, −9 °C. Manganese-depleted, spinach PSII preparations, which were identical to the samples utilized for fluorescence and EPR measurements, were partially dehydrated using a dry nitrogen stream; 30 μL of sample was placed between a CaF_2 and a Ge window (*14*, *17*, *23*). Immediately prior to dehydration, 3 mM potassium ferricyanide/3 mM potassium ferrocyanide or 48 mM potassium ferricyanide was added to the manganese-depleted PSII samples in HEPES and phosphate/formate buffers, respectively; the volumes of exogenous acceptors added to the samples were approximately equivalent. In the generation of difference FT-IR spectra, data were directly ratioed, on a noninteractive basis. For example, the "D3/D2" derived difference infrared spectrum corresponds to $\Delta A_{D3/D2} = A_{D3} - A_{D2}$. Difference spectra, obtained on PSII samples, were normalized to a 0.35 amide II absorbance and were an average of 50−60 spectra obtained on three different PSII preparations.

In the data collection for non-PSII-containing controls, an equivalent volume of the identical buffer (30 μL) was treated in the exact manner as the PSII samples above. Spectral conditions were as described above. Difference spectra, obtained on non-PSII-containing controls, were an average of 20−40 spectra.

To obtain amide I and II line shapes in some experiments (Figure 9), 2000 scans were coadded for each double-sided interferogram. Spectral conditions were as follows: resolution, 2 cm^{-1}; zero filling, one level; velocity, 2.5 cm/s; apodization function, Happ−Genzel; and temperature, −9 °C. Both manganese-depleted PSII and non-PSII controls were partially dehydrated, as above, before data acquisition. The FT-IR spectra of PSII samples were normalized to a 0.35 amide II absorbance.

Fluorescence Measurements. Measurements were performed on partially dehydrated, manganese-depleted PSII samples, using an Opti-Sciences OS-500 modulated fluorometer (Haverhill, MA). Samples were partially dehydrated onto a glass window. Immediately prior to drying, 3 mM

potassium ferricyanide/3 mM potassium ferrocyanide or 48 mM potassium ferricyanide was added to the manganese-depleted spinach PSII samples in HEPES and phosphate/formate buffers, respectively. Samples, which were identical to those used in EPR and FT-IR measurements, were illuminated via a red-filtered light source in the fluorometer. Spectral conditions for fluorescence yield measurements were as follows: modulation intensity, 180; saturation intensity, 180; time constant, 25 ms; scan time, 20 s; and illumination time, 20 s. Spectral conditions for the fluorescence decay measurements were as follows: modulation intensity, 180; saturation intensity, 180; time constant, 25 ms; and maximum allowable light pulse, 3 s. There was a 30 s interval between the pulses. Data shown were corrected for differences in protein concentration.

RESULTS

The tyrosyl D• radical in PSII is generated upon illumination and has a slow decay rate. These characteristics should permit facile observation of tyrosyl D• and its decay kinetics by infrared spectroscopy. Two different sets of biochemical conditions have been described for the observation of the infrared spectrum associated with tyrosine D oxidation (*10*, *11*, *14*−*19*). Under the first biochemical method, manganese-depleted photosystem II is maintained in 5 mM HEPES−NaOH (pH 7.5), which enhances the decay rate of tyrosyl D• (*6*), and 3 mM potassium ferricyanide/ferrocyanide is employed to reset the system between illumination events (*11*, *17*, *18*). Under the second biochemical method, manganese-depleted photosystem II is maintained in phosphate/formate buffer, containing 50 mM phosphate (pH 6.0) and 50 mM formate, and 48 mM potassium ferricyanide is employed as an electron acceptor (*10*, *19*).

Data Acquisition Scheme. In our previous vibrational studies on D and Z, we have employed two different data acquisition schemes. The first scheme utilized 4 min of continuous illumination and 4 min scan times and allowed us to acquire Z• − Z and D• − D spectra on the same sample (*11*, *15*−*18*). The second scheme utilized laser flashes to photoexcite PSII; the decay of the D• − D spectrum after the saturating flash was monitored (*17*). Control experiments showed that the acceptor side did not contribute to the spectra obtained (*11*, *15*−*18*). Here, we have used 20 s illumination and monitored the decay of tyrosyl radical D• after illumination.

In Figure 1, we present the data acquisition scheme used to acquire FT-IR and EPR spectra on manganese-depleted PSII membranes under both biochemical conditions. Samples were illuminated for 20 s with red-filtered light (Figure 1, L1). Following illumination, there was a 2 s pause before the initiation of data acquisition. Interferograms were acquired in 20 s intervals (Figure 1, D3-D5); after a 1 min pause, another 20 s interferogram was recorded (D6). After collection of D6, there was a pause in data acquisition to allow the further decay of the charge-separated state. Samples containing 5 mM HEPES−NaOH, pH 7.5 (HEPES PSII samples) were dark adapted for 90 min, whereas samples containing 50 mM phosphate and 50 mM formate, pH 6.0 (phosphate/formate PSII samples) were dark adapted for only 20 min, because D• decayed more rapidly under these conditions (*17*, *19*). Data acquisition then resumed with the acquisition of two interferograms, each acquired in 20 s (Figure 1, D1 and D2). The data acquisition cycle was iterated in order to average spectra. Additionally, samples were pre-illuminated before the beginning of data acquisition so that the first data acquisition cycle was identical to successive cycles.

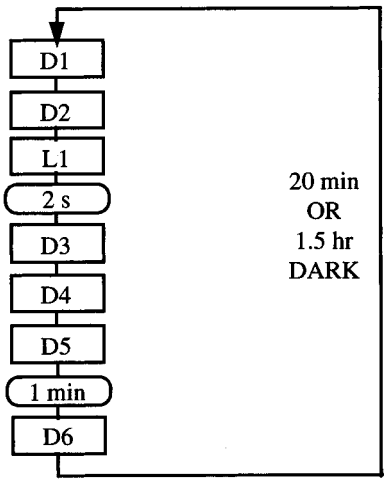

FIGURE 1: Data acquisition scheme for EPR and difference FT-IR experiments. The rectangular blocks correspond to 20 s of data acquisition. Within the schematic, "L" denotes illumination and "D" denotes dark.

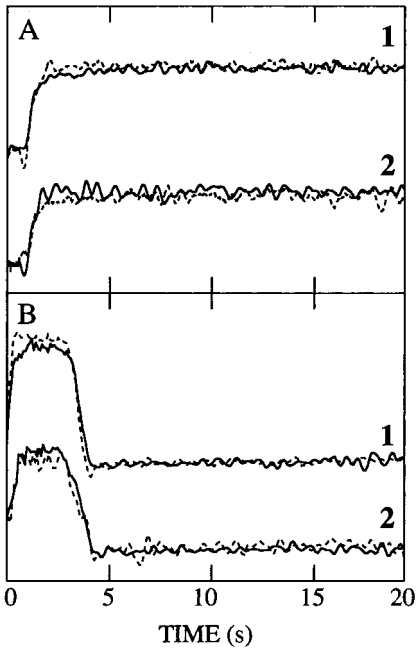

FIGURE 2: Fluorescence yield (A) and fluorescence decay measurements (B) on manganese-depleted, spinach PSII preparations. Data were obtained either on a HEPES PSII sample containing 5 mM HEPES−NaOH (pH 7.5), 3 mM potassium ferricyanide, and 3 mM potassium ferrocyanide (A and B, trace 1, solid lines) or on a phosphate/formate PSII sample containing 50 mM phosphate (pH 6.0), 50 mM formate, 10 mM NaCl, 15 mM $MgCl_2$, and 48 mM ferricyanide (A and B, trace 2, solid lines). Data were also obtained on the HEPES and phosphate/formate PSII samples containing 100 μM DCMU (A and B, traces 1 and 2, dashed lines).

Fluorescence Control Experiments. In Figure 2, we present fluorescence data used to monitor the yield and time dependence of fluorescence decay in the two PSII preparations during the data acquisition scheme. In the absence of fluorescence quenchers, such as P_{680}^+, the variable fluores-

cence serves as a indirect measure of the yield and decay of Q_A^- (*24*). Data were acquired on HEPES PSII samples containing 3 mM potassium ferricyanide and 3 mM potassium ferrocyanide (Figure 2, A and B, line 1) or on phosphate/formate PSII samples containing 48 mM potassium ferricyanide (Figure 2, A and B, line 2). Samples were partially dehydrated on a solid substrate and were illuminated with red-filtered light. These are the conditions that will be employed for FT-IR spectroscopy.

The data in Figure 2A show the accumulation of variable fluorescence and thus Q_A^-, under continuous illumination for 20 s in both PSII samples. The data support the conclusion that the yield of Q_A^-, produced under continuous illumination, was similar in the HEPES and phosphate/formate PSII samples (Figure 2A, solid lines 1 and 2). In Figure 2B, we present the time dependence of the variable fluorescence decay and, thus, the time dependence of Q_A^- decay. In both samples, Q_A^- decayed completely in the first second following the cessation of illumination (Figure 2B, solid lines 1 and 2). Both the yield of Q_A^- and the decay were not altered in the presence of DCMU, an inhibitor of electron transfer between Q_A and Q_B (Figure 2, A and B, dotted lines 1 and 2). This last observation indicates that the Q_B is not acting as an electron acceptor under these conditions (for example, see ref *25*).

Reexamination of the data acquisition scheme shown in Figure 1 leads to the following conclusions. First, Q_A^- is formed under illumination in PSII membranes (Figure 1, L1), but the semiquinone anion radical will decay in the 2 s pause before data acquisition begins both in HEPES and in phosphate/formate samples (Figure 1, D3−D6). Therefore, the $Q_A^- - Q_A$ infrared spectrum will not contribute to infrared data used to construct the D3/D2, D4/D2, D5/D2, or D6/D2 difference infrared spectrum (Figure 1). Second, in either HEPES or phosphate/formate samples, redox changes involving Q_B will also not be observed.

EPR Control Experiments. In Figure 3, we present EPR data acquired as a function of time after illumination. Data were obtained either on HEPES PSII samples containing 3 mM potassium ferricyanide/ferrocyanide or on phosphate/formate PSII samples containing 48 mM potassium ferrocyanide. Each sample was partially dehydrated on a solid substrate, and the illumination source was red- and heat-filtered. These are the same conditions as will be employed for FT-IR spectroscopy. Samples were illuminated for 20 s and, following a 2 s pause, spectra were obtained in 20 s sweeps, duplicating the infrared collection scheme shown in Figure 1. The repetition rate for HEPES samples was one cycle every 90 min, and for phosphate/formate samples it was one cycle every 20 min. As expected, under illumination, an increase in amplitude of the EPR signals of tyrosyl radicals D• and Z• was observed. Also, as expected (see, for example, ref *17*), tyrosine Z• decayed in the 2 s pause before the beginning of data acquisition (data not shown).

In Figure 3A, we present data showing the decay of tyrosyl radical D• as a function of time after illumination, as assessed by EPR spectroscopy. As shown, the decay of D• was slower in HEPES PSII samples (Figure 3A, circles), when compared to the decay of D• in phosphate/formate PSII samples (Figure 3A, triangles). Biexponential decay kinetics were observed in both preparations (Figure 3A). In Figure 3A, each EPR data set was normalized independently to the D• yield, obtained 2 s after illumination (D3, Figure 1). A quantitative comparison of EPR spectra, obtained on phosphate/formate and HEPES PSII, showed that the yield of D•, obtained in phosphate/formate PSII, was only 25 ± 5% of the yield of D• in HEPES PSII (as assessed 2 s after illumination). We conclude that the phosphate/formate buffer decreases the yield and accelerates the decay rate of tyrosyl radical, D•.

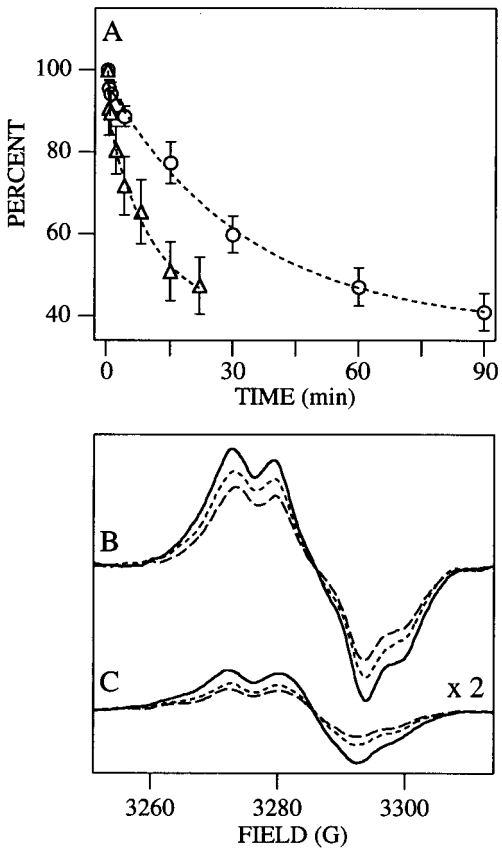

FIGURE 3: (A) Decay of tyrosyl radical D•, as assessed by EPR spectroscopy, in HEPES PSII (circles) or phosphate/formate PSII (triangles). Each set of data was normalized independently to the number of D• spins in the D3 spectrum (see Figure 1). The best biexponential fit to the average of the data points is shown. (B, C) Difference EPR spectra obtained on manganese-depleted spinach PSII preparations. Data shown in (B) and (C) were obtained on HEPES PSII or phosphate/formate PSII samples, respectively. Data were corrected for any differences in gain and chlorophyll concentration between the two types of samples, and then the spectra shown in (C) were multiplied by a factor of 2, to facilitate comparison. In each panel, field-swept EPR spectra were acquired by the data acquisition scheme shown in Figure 1. For (B), spectra were obtained 2 s (D3), 22 s (D4), 44 s (D5), and 90.3 min (D2) after a 20 s illumination, whereas for (C), spectra were obtained 2 s (D3), 22 s (D4), 44 s (D5), and 20.3 min (D2) after a 20 s illumination. In (B) and (C), difference EPR spectra were derived by subtraction and correspond to D3/D2 (D3 − D2, solid line), D4/D2 (D4 − D2, dotted line), and D5/D2 (D6 − D2, dashed line). Spectral conditions were as follows: frequency, 9.21 GHz; microwave power, 0.8 mW; modulation amplitude, 3.5 G; scan time, 20 s; time constant, 0.7 s; and temperature, −9 °C.

In Figure 3, B and C, we present difference EPR spectra constructed from the 20 s field-swept data obtained on HEPES PSII and phosphate/formate PSII samples, respectively. These data were obtained by subtraction of the appropriate EPR spectra (Figure 1). For example, to construct the "D3/D2" difference spectrum (Figure 3, B and C, solid line), data obtained during the interval, D2, were

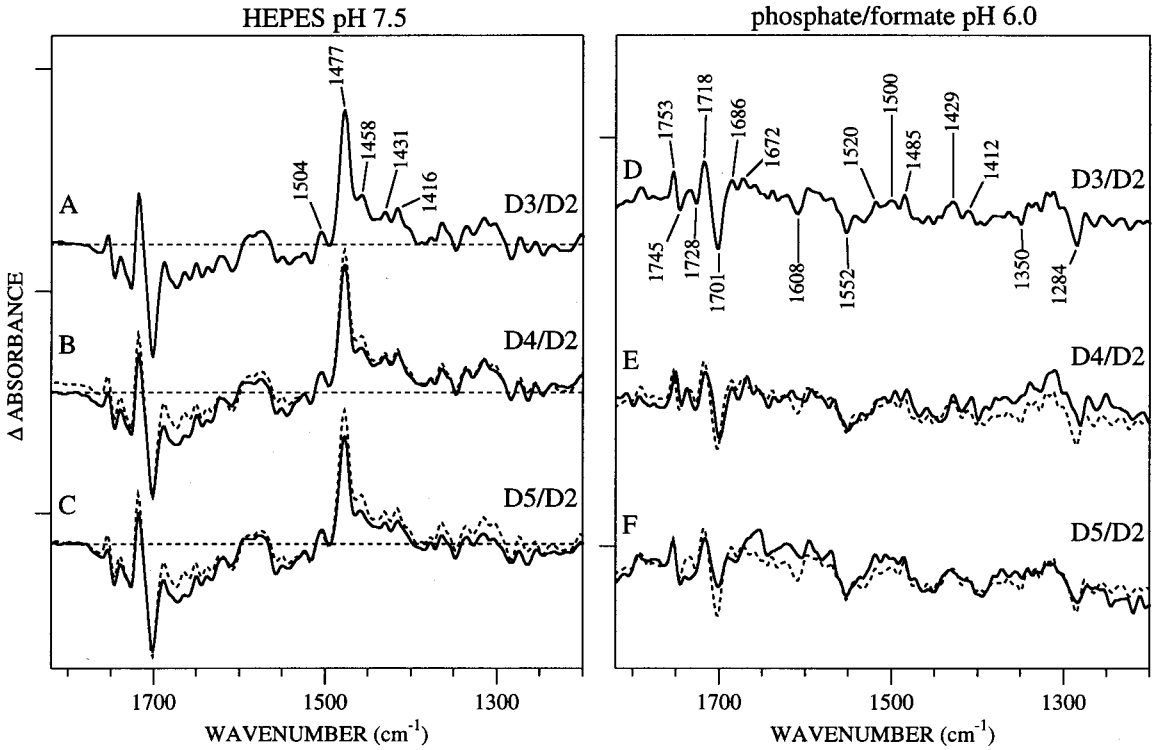

FIGURE 4: Difference FT-IR spectra obtained on manganese-depleted spinach PSII, reflecting D• − D. Data shown in (A−C) and (D−F) were obtained on HEPES PSII or phosphate/formate PSII samples, respectively. Spectra were acquired by the data acquisition scheme shown in Figure 1. Spectra shown in solid lines in (A) and (D), in (B) and (E), and in (C) and (F) correspond to the D3/D2 (D3 − D2), D4/D2 (D4 − D2), and D5/D2 (D5 − D2) difference FT-IR spectra, respectively. The spectra shown in (A) and (D) are superimposed as dashed lines in (B) and (C) and (E) and (F), respectively. Data shown in (A−C) are an average of 57 spectra, and data shown in (D−F) are an average of 60 spectra. Tick marks on the *y* axis are 2×10^{-4} AU; notice that the left and right panels are not on the same *y* scale.

subtracted from data obtained during the interval, D3 (Figure 1). The data shown in Figure 3, B and C, correspond to difference spectra, called D3/D2 (D3 − D2, solid line), D4/D2 (D4 − D2, dotted line), and D5/D2 (D5 − D2, dashed line). In both samples, the spectra represent the rate of tyrosyl radical D• decay over the 60 s following illumination (Figure 3, B and C). In phosphate/formate samples (Figure 3C), the yield of D•, as assessed by difference EPR spectroscopy 2 s after illumination, was 16% of the D• yield in HEPES samples (compare Figure 3, B and C, solid line). Double integration of these difference EPR spectra will predict the amount of D• decay in the corresponding FT-IR experiments (see below).

On the basis of these fluorescence and EPR control experiments, we conclude that D3/D2, D4/D2, and D5/D2 difference FT-IR spectra (Figure 1) will reflect a contribution from D• − D and that these spectra will be free of contributions from reduction of Q_A and Q_B. Moreover, D• − D contributions will be obtained in both types of PSII samples. Infrared spectroscopy can be employed to elucidate the origin of the lower D• yield and faster D• decay in phosphate/formate PSII, as the technique can probe alterations in protein structure.

FT-IR Measurements. In Figure 4, we present difference FT-IR data acquired as a function of time after illumination. Data were obtained from HEPES PSII samples (Figure 4, A−C) and from phosphate/formate PSII samples (Figure 4, D−F). Fluorescence measurements on phosphate/formate samples showed that Q_A^- decayed before the beginning of data acquisition and that Q_B was not functional as an electron acceptor, whereas EPR measurements demonstrated that D• decayed over the time used to acquire FT-IR data. Thus, data acquisition using the protocol in Figure 1 would be expected to reflect tyrosyl D• decay in both phosphate/formate PSII and HEPES PSII samples.

As expected from our previous studies of more highly resolved spinach and cyanobacterial PSII core preparations (*17*), the FT-IR spectra, obtained on HEPES PSII samples, exhibited an intense positive line at 1477 cm^{-1}, which decayed as a function of time after illumination (Figure 4, A−C). In agreement with our previous body of work, the 1477 cm^{-1} line is assigned to tyrosyl radical, D• (*17*, *18*). Assignment of the 1477 cm^{-1} line to D• was supported by the quantitative comparison of infrared and EPR decay kinetics in Figure 5A. The data superimposed within the signal-to-noise of the two measurements (Figure 5A) and also coincided with the decay of the positive 2113 cm^{-1} band of potassium ferricyanide (*26*). Note that a negative band at 1701 cm^{-1} also decayed with the same kinetics (Figure 5A); tyrosine labeling experiments have provided evidence for a tyrosyl radical/tyrosine contribution in this spectral region (*18*). These results support the assignment of the 1477 cm^{-1} spectral feature to tyrosyl D• radical in spinach photosystem II membranes, as expected from our studies of more highly resolved preparations (*17*).

Figure 4, D−F, shows the difference FT-IR spectra acquired, as a function of time after illumination, on phosphate/formate PSII samples. As predicted by EPR control experiments on phosphate/formate PSII (Figure 3C), the spectra were reduced markedly in amplitude, compared to spectra obtained on HEPES PSII (Figure 4, A−C). Frequency shifts and changes in intensity were also observed.

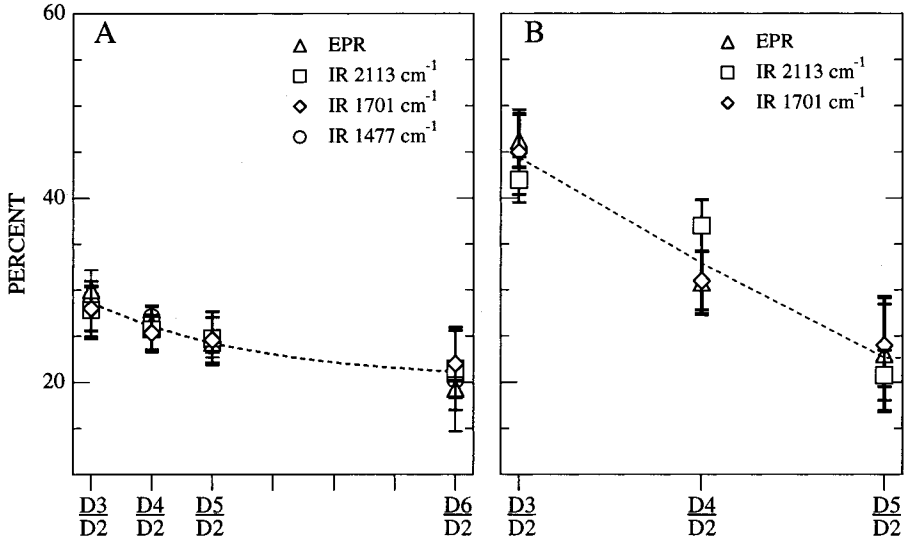

FIGURE 5: (A) Decay of tyrosyl D• signals, as assessed by EPR and FT-IR spectroscopy, in HEPES PSII samples. Data plotted are derived by double integration of the difference EPR spectra shown in Figure 3B (△), and from the amplitudes of the positive 2113 cm^{-1} (□), the negative 1701 cm^{-1} (◇), and the positive 1477 cm^{-1} (○) vibrational lines in the difference infrared spectra shown in Figure 4, A−C. (B) Decay of tyrosyl D• signals, as assessed by EPR and FT-IR spectroscopy, in phosphate/formate PSII samples. Data plotted are derived by double integration of the difference EPR spectra shown in Figure 3C (△) and from the amplitudes of the positive 2113 cm^{-1} (□) and the negative 1701 cm^{-1} (◇) signals in the difference infrared spectra shown in Figure 4, D−F. Each set of EPR and FT-IR data was independently normalized to the total amount of decay obtained, to facilitate comparison. The scale on the *y* axis is the same in (A) and (B). The best monoexponential fit to the average of the data points is shown as the dotted line.

In particular, these data exhibited no observable 1477 cm^{-1} line in any difference spectrum that was obtained during this 60 s time regime (Figure 4, D−F). These spectra bear resemblance to the FT-IR data previously reported under these conditions (*10*, *19*); the frequencies agree, on average, within ±14 cm^{-1}. For example, there is a 1500 cm^{-1} line in the difference infrared data reported here, obtained on phosphate/formate PSII, which may be equivalent to the 1504 cm^{-1} line in (*19*). The greatest disparity, between the infrared spectra on phosphate/formate PSII samples reported here (Figure 4) and in ref *19*, is in the amide I region (1680−1630 cm^{-1}). Note that the data of ref *19* were obtained at 4 °C, while our experiments were conducted at −9 °C. This temperature difference may explain the minor spectral differences observed. The 4 °C experiments of ref *19* involved the disadvantage of much longer incubation times in phosphate/formate buffer, which has the potential to give rise to alterations in the spectra over the course of data acquisition. This difference in data acquisition protocol may explain the spectral differences obtained.

Evaluation of the Alternate FT-IR Spectrum in Phosphate/Formate PSII Samples. As discussed in ref *17*, the failure to observe the 1477 cm^{-1} line of D• and other spectral alterations observed in phosphate/formate-containing PSII samples could be caused by several possible effects. First, use of a time regime where D• spectral contributions cancel in the difference spectrum could have been the origin of this observation (*19*). However, this possibility cannot explain the results presented here, because we have monitored the time-dependent decay of the difference infrared spectrum and have not observed a 1477 cm^{-1} line. Second, the decrease in the amount of charge separation and/or increased aggregation under these conditions could make the vibrational modes of D• undetectable. Third, phosphate/formate may have the effect of shifting or canceling the vibrational lines of D•, either because phosphate/formate contributes to the spectrum or because phosphate/formate exerts a direct effect on the environment of tyrosine D.

To evaluate the possibility that the altered vibrational lines arise from tyrosine D• in phosphate/formate PSII samples, a quantitative comparison of the EPR and FT-IR derived kinetics was performed. In Figure 5B, we plot the decay of a positive band at 2113 cm^{-1}, which arises from potassium ferricyanide (*26*), versus the decay of tyrosyl D•, as assessed by EPR spectroscopy on phosphate/formate samples. The two measurements coincided, given the signal-to-noise of the two measurements (Figure 5B). This result supports the overall conclusion that some of the FT-IR spectral changes observed arise from redox changes involving tyrosyl radical D•. The agreement was not as obvious for bands in the 1600−1400 cm^{-1} region, perhaps because of the small amplitude of the observed signals relative to the baseline, which exhibited interference fringes that also changed as a function of time. Interference fringes are a consequence of performing infrared spectroscopy in transmission mode and cannot be eliminated. However, the amplitude of a more intense, negative line at 1701 cm^{-1} was plotted in Figure 5B, and this more intense band decayed with kinetics, which superimposed on the decay of the ferricyanide band and the decay of the EPR signal (Figure 5B). The negative 1701 cm^{-1} line, observed in spectra obtained on HEPES samples, showed the same behavior (Figure 5A).

As an additional control, we performed a quantitative comparison of EPR and FT-IR amplitudes. The overall intensity of spectral features observed, for example, at 1485 cm^{-1}, was approximately 10% of the spectral amplitudes observed in HEPES samples (Figure 6A, solid and dashed lines). Given the small amplitude of both EPR and FT-IR signals, this decrease in amplitude was similar to the decrease observed in D• yield, which we have measured via EPR spectroscopy (Figure 3).

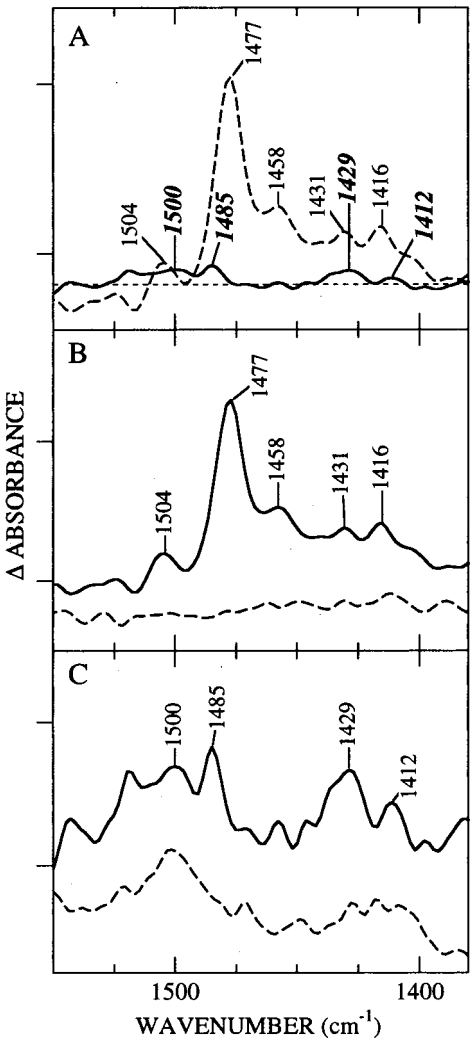

FIGURE 6: Difference FT-IR spectra obtained on manganese-depleted spinach PSII, reflecting $D^{\bullet} - D$, and on buffer controls. In (A), difference spectra were obtained on HEPES PSII (dashed line, D3/D2, which is repeated from Figure 4A) and on phosphate/formate PSII (solid line, D3/D2, which is repeated from Figure 4D). These data are shown superimposed and on the same scale to facilitate comparison of relative amplitudes. In (B), difference spectra were obtained on HEPES PSII (solid line, D3/D2, which is repeated from Figure 4A) and on the HEPES-containing buffer plus 3 mM potassium ferricyanide/3 mM potassium ferrocyanide, lacking PSII (dashed line, D3/D2). In (C), difference spectra were obtained on phosphate/formate PSII (solid line, D3/D2, which is repeated from Figure 4D) and on the phosphate/formate-containing buffer plus 48 mM potassium ferricyanide, lacking PSII (dashed line, D3/D2). Tick marks on the *y* axis are 1×10^{-4} (A), 1.0×10^{-4} (B), and 0.2×10^{-4} (C) AU.

Next, we evaluated the possibility that phosphate and formate contribute directly to the difference spectrum. This was performed using control experiments in which PSII was omitted from the sample. The results are shown in Figures 6 and 7. Solutions, containing 5 mM HEPES−NaOH (pH 7.5), 3 mM potassium ferricyanide, and 3 mM potassium ferrocyanide but lacking PSII, gave the expected result, i.e., no defined spectral features in any spectral region in the light-minus-dark difference spectrum (Figure 6B, dashed line, and Figure 7A). On the other hand, solutions containing phosphate/formate buffer and 48 mM potassium ferricyanide, but lacking PSII, gave well-defined spectral changes (Figure 6C, dashed line, and Figure 7B). We attribute these spectral changes, which occur over the time course of data acquisition

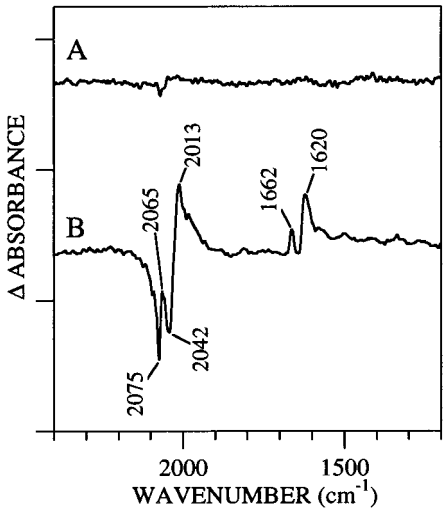

FIGURE 7: Difference FT-IR spectra obtained on buffer controls. In (A), spectra were obtained on the HEPES-containing buffer plus 3 mM potassium ferricyanide/3 mM potassium ferrocyanide, lacking PSII (D3/D2, repeated from Figure 6B). In (B), spectra were obtained on the phosphate/formate-containing buffer containing 48 mM potassium ferricyanide, lacking PSII (D3/D2, repeated from Figure 6C). Tick marks on the *y* axis are 2.0×10^{-4} AU.

in this solution, to slow rearrangements in the coordination shell of Fe(III) in potassium ferricyanide when formate and phosphate are present (*27*). Ferricyanide is labile to such ligand rearrangement reactions; phosphates and carboxylates are known to coordinate Fe(III) (*27*). The changes in the CN stretching region (2200−2000 cm^{-1}) support this interpretation (Figure 7B).

Notice that in the region from 1550 to 1380 cm^{-1}, a band at 1500 cm^{-1} was observed in phosphate/formate/ferricyanide solutions lacking PSII (Figure 6C, dashed line). Ferricyanide has no fundamental vibrations in the 1800−1200 cm^{-1} region (*26*), so these vibrational lines are attributed to phosphate/formate. This buffer band at 1500 cm^{-1} was also observed, with similar intensity, in spectra obtained on phosphate/formate PSII samples (Figure 6C, solid line).

However, there were spectral features, observed in phosphate/formate PSII samples, which were not observed in the difference spectra of the buffer (Figure 6C, compare solid and dashed lines). The 1485 cm^{-1} line is an example of such a spectral feature. We conclude that some spectral features, observed in phosphate/formate PSII samples, arise from buffer components, but that some arise from redox changes involving tyrosine D. Therefore, the most likely explanation of the altered FT-IR spectrum, observed in phosphate/formate PSII samples, is that phosphate/formate contributes directly to the spectrum and that phosphate/formate alters the vibrational spectrum associated with the reduction of tyrosine $D^{\bullet}$.

Origin of Phosphate/Formate Effects. To understand the origin of the spectral alterations observed in the presence of the phosphate/formate buffer, the amide I line shapes of the FT-IR derived absorption spectra were examined in HEPES and phosphate/formate PSII samples. The amide I vibration arises from the C═O stretching mode of the peptide bond (*28*). Changes in secondary structure result in alterations in the infrared amide I line shape (reviewed in refs *29*−*31*).

In Figure 8, we present the 1850−1420 cm^{-1} region of FT-IR absorption spectra; these data were used in construct-

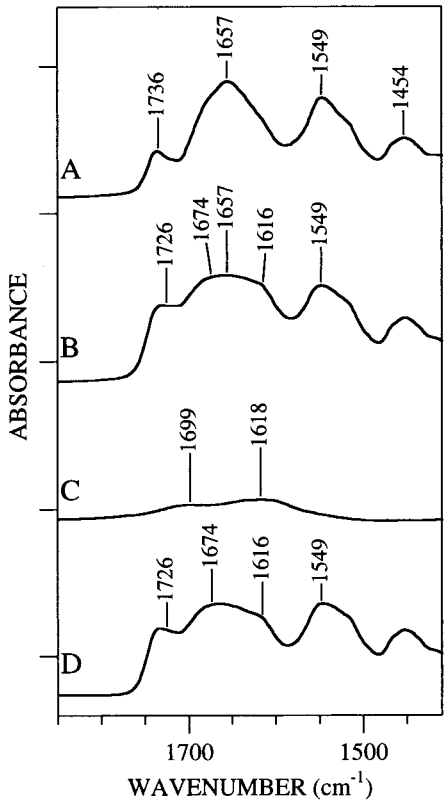

FIGURE 8: Infrared absorption spectra obtained on (A) HEPES PSII samples, (B) phosphate/formate PSII samples, and (C) the phosphate/formate buffer, containing 50 mM phosphate (pH 6.0), 50 mM formate, 10 mM NaCl, 15 mM $MgCl_2$, and 48 mM ferricyanide. The spectrum shown in (D) was obtained as the result of subtraction of (C) from (B) and represents the amide I line shape of PSII, after treatment with phosphate and formate. Tick marks on the *y* axis are 0.5 AU. These data were used in constructing the difference FT-IR spectra shown in Figure 4, and are an average of two to six spectra, obtained in the dark.

ing the difference spectra shown in Figure 4. In Figure 8A, we show the amide I line shape of PSII obtained in HEPES buffer. The amide I band was relatively narrow, with a peak at 1657 cm^{-1}. This frequency is characteristic of α helical proteins (reviewed in refs *29*−*31*). Minor amide I components at higher and lower frequency were also observed (Figure 8A). These results were in reasonable agreement with earlier studies of the secondary structure of PSII (for example, see refs *32*).

However, the amide I line shape of PSII membranes in phosphate/formate buffer was perturbed (Figure 8B). Because the concentration of phosphate and formate was relatively high in these samples (50 mM), spectra were obtained of the phosphate/formate buffer alone, in the absence of PSII (Figure 8C), as a control. This spectrum, representing the buffer components, was subtracted from the spectrum of the phosphate/formate PSII sample. The subtraction result (Figure 8D) showed an altered amide I line shape for PSII and confirmed that the altered amide I line shape was not the result of phosphate and formate contributions to the 1650 cm^{-1} spectral region. As support for the conclusion that the amide I line shape is altered in phosphate/formate buffer, notice that accompanying alterations in the amide II region (approximately 1550 cm^{-1}) were also observed (Figure 8, A and D).

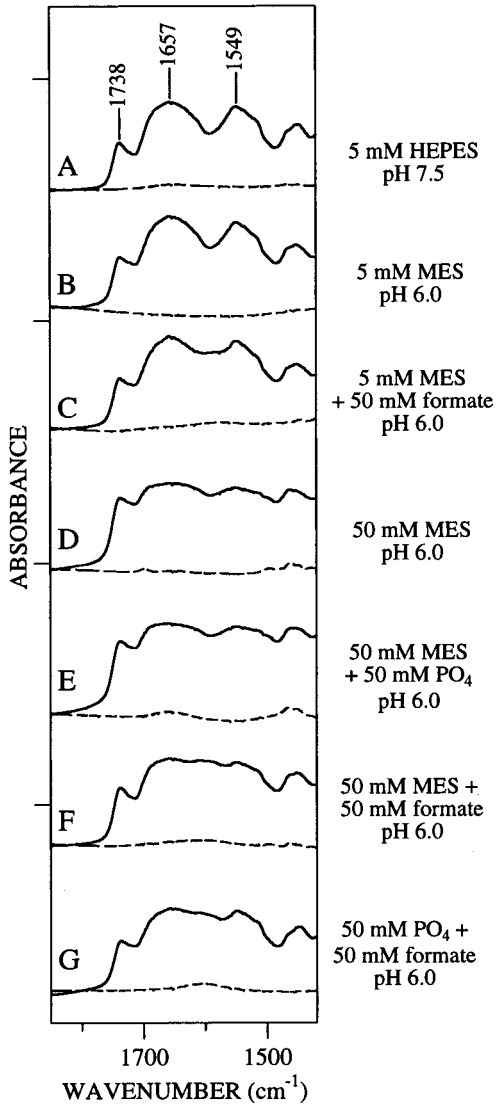

FIGURE 9: Infrared absorption spectra obtained on PSII samples and buffer controls. The solid lines correspond to data obtained on PSII in (A) 5 mM HEPES−NaOH (pH 7.5), (B) 5 mM MES−NaOH (pH 6.0), (C) 5 mM MES−NaOH (pH 6.0) and 50 mM formate, (D) 50 mM MES−NaOH (pH 6.0), (E) 50 mM MES−NaOH (pH 6.0) and 50 mM phosphate, (F) 50 mM MES−NaOH (pH 6.0) and 50 mM formate, and (F) phosphate/formate buffer containing 50 mM phosphate (pH 6.0), 50 mM formate, 10 mM NaCl, and 15 mM $MgCl_2$. The dashed lines in (A−F) correspond to data obtained on the buffer alone, as defined above for (A−F). These spectra were obtained at a spectral resolution of 2 cm^{-1} (see Materials and Methods). The tick marks on the *y* axis are 1.0 AU.

Biochemical Dissection of the Phosphate/Formate Effect. The results in Figure 8 demonstrated that the amide I line shape of phosphate/formate PSII samples was dramatically altered, when compared to the line shape observed in HEPES samples. These data suggested a gross structural rearrangement of PSII. To identify the origin of the amide I change, buffer conditions were varied independently. Figure 9 shows the results of this experiment. The amide I line shapes of PSII, suspended in either 5 mM HEPES−NaOH, pH 7.5, or 5 mM MES−NaOH, pH 6.0, were indistinguishable (Figure 9, A and B). From these data, we conclude that a change in pH from pH = 7.5 to pH = 6.0 does not perturb the secondary structure of PSII. These are the usual conditions that we employ for difference FT-IR spectroscopy on PSII

Table 1: Effects of Phosphate and Formate on the Yield and Decay of Tyrosyl Radical, D• [d]

PSII	sample conditions[a]	D• spins[b]	% decay[c]
A	MES, ferricyanide	1.00	42
B	MES, phosphate, ferricyanide	1.06	45
C	MES, formate, ferricyanide	0.64	65

[a] When present, the MES concentration was 50 mM MES−NaOH (pH 6.0), the potassium ferricyanide concentration was 48 mM, the phosphate concentration was 50 mM, and the formate concentration was 50 mM. [b] The EPR spectrum was acquired following a 20 s illumination and a 2 s dark adaptation. This spectrum corresponds to spectrum D3 in Figure 1. The data were normalized to the number of spins obtained in sample A. [c] The EPR spectrum was obtained after a 90 min dark adaptation, which followed the 20 s illumination. The data were normalized to the number of spins obtained 2 s following illumination. The percent decay was then computed by subtraction from 100%. [d] Spin quantitations of tyrosyl D• EPR spectra obtained on manganese-depleted, spinach PSII preparations. Quantitations were performed by double integration of the EPR spectra and by correction for differences in gain and chlorophyll concentration. The standard error is estimated as approximately 10%.

(for example, see refs *11*, *17*, *18*). An increase in ionic strength at pH 6.0, from a 5 mM MES (Figure 9B) to a 50 mM MES concentration (Figure 9D), led to amide I line shape alterations in PSII. Addition of 50 mM formate (Figure 9, C and F) but not 50 mM phosphate (Figure 9E) gave additional, small spectral changes. The amide I and amide II line shapes obtained on PSII samples in 50 mM MES−NaOH, pH 6.0, and 50 mM formate (Figure 9F) closely resembled data obtained on phosphate/formate PSII samples (Figure 9G).

We conclude that at pH 6.0, a protein conformational change occurs when PSII is incubated in high ionic strength buffers. We attribute the majority of this change to a possible electrostatic effect on the structure of PSII, resulting from differences in ionic strength between the HEPES (*11*, *17*, *18*) and phosphate/formate (*19*) buffers employed. Note that these samples were partially dehydrated, which would also increase the effective ionic strength. Smaller effects on the structure of PSII may arise from the presence of formate. The above observation of an electrostatic effect on PSII structure is consistent with crystallographic studies of the multisubunit immunoglobulin light chain (*33*). In this work, three quaternary structures for the immunoglobin light chain were obtained; the quaternary structure depended on the identity of the crystallization solvent (*33*).

We also examined the impact of various buffer components on PSII EPR spectra. To identify the origin of the decrease in yield and of the acceleration in the decay rate of D•, as assessed by EPR spectroscopy, buffer conditions were varied independently. Table 1 gives the relative yield of D•, as assessed by double integration of the EPR spectrum obtained 2 s after illumination (corresponding to D3 in Figure 1). Table 1 also presents data concerning the decay rate of D•, as assessed by double integration of the spectrum obtained 90 min after illumination. The addition of 50 mM formate was shown to decrease the yield of D•, obtained 2 s after illumination, and increase the rate of decay of the radical over the 90 min following illumination (Table 1). The decay rate was dependent on the potassium ferricyanide concentration, suggesting that formate was not acting as a donor but was facilitating the reduction of tyrosyl radical D• by another donor (data not shown). We conclude that formate can decrease the yield of D• and can accelerate the rate of D• decay in PSII.

DISCUSSION

In this report, time-resolved difference FT-IR spectra, associated with the reduction of tyrosine D•, have been obtained from spinach photosystem II membranes, as isolated by the method of ref *21*. Conditions were employed (5 mM HEPES−NaOH, pH 7.5; 3 mM potassium ferricyanide/ferrocyanide) in which Q_A^- was shown to decay in the 2 s before data acquisition began, but tyrosine D• decayed significantly over the 60 s time scale of the FT-IR measurements. Our experiments support the conclusion that tyrosyl radical, D•, gives rise to an intense spectral feature at 1477 cm^{-1}. Superposition of kinetic transients, derived from infrared and EPR analysis, provides the foundation for this assignment. These results are in agreement with our previous work, in which isotopic labeling, site-directed mutagenesis, and superposition of kinetic transients were used to assign the positive 1477 cm^{-1} line to tyrosyl radical D• in more highly resolved PSII preparations at pH 7.5 (*17*, *18*).

In our previous work (*17*, *18*), comparison of spectra obtained on preparations in which tyrosine was ^{13}C or ^{2}H labeled led to the assignment of the 1477 cm^{-1} line to the C−O vibration of tyrosyl radical, D•. The 1477 cm^{-1} frequency of this vibrational feature is downshifted by 20−30 cm^{-1} from the typical C−O frequencies observed for tyrosyl and phenoxyl radicals in vitro (*34*, *35*). Upshifts of the frequencies of negative lines, which were sensitive to tyrosine labeling, were also observed (*18*). As a first speculative explanation for the observed downshift of the C−O vibration of D•, we proposed that nonbonding interactions involving peptide formation and perhaps details of peptide conformation at tyrosine D may shift the C−O frequency. As a second possible explanation, we proposed that the generation of charged species in a hydrophobic environment may generate electric fields, which shift vibrational frequencies (*17*, *18*).

An alternative assignment of the spectral feature at 1477 cm^{-1} to Q_A^- has been made; this assignment was not based on isotopic labeling, however (*13*, *36*). Many published experimental observations are inconsistent with this assignment (reviewed in ref *17* and see also ref *11*, *12*, *14*−*16*, *18*, *37*, *38*), including the observations described here. Note that preliminary data, obtained as a result of isotopic labeling of plastoquinone, also do not support the conclusion that Q_A^- contributes significantly to the 1477 cm^{-1} line (Razeghifard, Steenhuis, Kim, and Barry, unpublished results).

We have obtained an alternate difference FT-IR spectrum in phosphate/formate-containing PSII samples, which is similar to previous reports of an alternate D• − D spectrum (*10*). We have confirmed that tyrosyl radical D• decay is occurring over the time scale where FT-IR data are acquired; however, the yield of D• is reduced dramatically in phosphate/formate PSII samples, relative to the HEPES PSII samples. Difference infrared spectra, obtained in this time regime, show alterations in both amplitude and frequency and do not exhibit a 1477 cm^{-1} line. The decrease in amplitude of the vibrational spectrum is approximately proportional to the decrease in D• EPR yield. Superposition of EPR-derived transients and FT-IR amplitudes supports the conclusion that

some of the observed spectral features arise from redox changes involving tyrosine D. When difference FT-IR spectra, obtained on HEPES and phosphate/formate PSII, are compared, alterations in frequency are observed throughout the vibrational spectrum. While some of these altered vibrational lines arise because of phosphate/formate contributions to the spectrum, this observation cannot explain all of the spectral changes observed. Therefore, we conclude that phosphate/formate conditions alter the structure and/or environment of tyrosine D and, thus, alter the vibrational spectrum associated with D• reduction.

We attribute the altered vibrational spectrum, associated with D• reduction, in part to a large-scale structural rearrangement in PSII. These effects may explain, in part, the decrease in yield of the tyrosyl radical. Other infrared studies have shown a correlation of amide I line shape changes with inhibitory effects (*32*, *39*, *40*). The new frequencies at 1674 and 1616 cm^{-1}, observed in the FT-IR absorption spectrum of phosphate/formate PSII, are in the spectral ranges most often assigned to β sheet (*29*−*31*). Two high- and low-frequency components are expected as the result of transition dipole coupling (*28*). A low 1616 cm^{-1} component has been observed as a result of intermolecular hydrogen bonding in protein samples (*41*). A conversion of α helical to β sheet structure is a large-scale conformational rearrangement, and such changes can be caused by the binding of anions to proteins (*42*, *43*). This conformational rearrangement may be due primarily to an ionic strength effect on PSII structure.

Our experiments have also shown that 50 mM formate lowers the yield and accelerates the rate of decay of tyrosyl radical, D•. Our previous work, employing chemical complementation, provides an explanation of a possible mechanism by which formate influences the properties of tyrosine D (*11*). In those experiments, imidazole was shown to have access to tyrosine D in wild-type PSII and in a histidine to leucine mutant, generated in the environment of tyrosine D. To explain the access of imidazole to tyrosine D, we modeled the three-dimensional structure surrounding redox-active tyrosine D. This modeling was based on similarities to the bacterial reaction center. This work provided evidence for a surface-accessible pocket near the redox-active tyrosine (*11*). If imidazole has access to tyrosine D in wild-type PSII, then other buffer components may have access as well. The accelerating effect of formate on D• reduction is opposite to the retarding effect of imidazole on this electron-transfer step in wild-type (*11*). These effects on the electron-transfer rate may be associated with the generation of charged species and electric fields in the hydrophobic environment of D. The magnitude and direction of the electric field may play a role in controlling the direction and rate of electron transfer (for example, see ref *44*).

Our work has also shown that in phosphate/formate buffers, shifts are observed in the frequencies of lines associated with reduction of tyrosyl radical, D•. For example, the 1477 cm^{-1} line may be upshifting to 1485 cm^{-1}; isotopic labeling is required to test this hypothesis. Frequency shifts in the presence of a high concentration of anionic compounds may be consistent with the hypothesis that electric field effects are responsible for the perturbations of the D• − D vibrational spectrum (*17*, *18*). Such large spectral shifts were not observed when imidazole was present in wild-type PSII (*11*). However, the total concentration of imidazole employed was low in those experiments (1 mM). On the other hand, another possible explanation for the failure to observe the 1477 cm^{-1} line in phosphate/formate is that strong hydrogen bonding takes place between buffer components and D•. Strong hydrogen bonding could broaden the C−O vibrational mode (ν_{7a}) of the radical and could make this line undetectable (*45*). Note that in addition to perturbations of positive lines in the radical's vibrational spectrum, perturbations to negative lines, possibly derived from the tyrosine, are observed as well. For example, the negative 1284 cm^{-1} line, observed in spectra of phosphate/formate PSII, is not observed in spectra of HEPES PSII (*18*). This perturbation may be an indicator of a change in the hydrogen-bonding status or the protonation state of tyrosine D.

Taken together, the FT-IR results are consistent with an environmental alteration, which affects the structure and function of tyrosyl radical, D•, and tyrosine D. Our results also suggest that environmental factors can have a relatively large effect on the vibrational spectrum of D• and, yet, have only a small or negligible effect on the EPR line shape of the radical. This is possible because the D• EPR line shape is broadened by anisotropic interactions and is relatively insensitive to small changes in hydrogen-bonding and other types of nonbonding effects (*46*).

The alternate D• − D spectrum (*10*) has been observed in cyanobacterial PSII preparations, which have also been treated with phosphate and formate buffers. These spectra resemble spectra obtained from spinach PSII membranes, which have been treated with phosphate/formate (*19*). In the D• − D spectrum obtained on a phosphate/formate cyanobacterial sample, spectral changes observed upon ^{13}C labeling of tyrosine at C_1 of the phenol ring were used to argue that the 1503 cm^{-1} arises from D• (*10*) (but see discussion of these results in ref *17*). The data, which we have presented here, show that the phosphate/formate buffer also makes a contribution at 1500 cm^{-1}; this will complicate the interpretation of isotope-shifted spectra. Indeed, as previously discussed, the lack of observed isotope shift at 1503 cm^{-1} upon $^{13}C_6$ labeling of the tyrosine ring was problematic in the interpretation of the isotope shifts (*10*, *17*).

Assignment of the Z• − Z spectrum is also of interest. MacDonald et al. recorded the vibrational spectrum of Z• and suggested the assignment of a positive 1478 cm^{-1} line to the C−O vibration, based on isotopic labeling (*15*). Our more recent work on Z• has tested and confirmed this assignment (*16*−*18*). Recently, an alternate spectrum has been assigned to Z• − Z; this spectrum lacks a 1478 cm^{-1} line (*47*). Spectra were obtained on PSII in a buffer containing 50 mM MES (pH 6.0), 10 mM NaCl, 5 mM $MgCl_2$, approximately 10 mM sorbitol, and approximately 100 mM potassium ferricyanide. Data were obtained in 3.6 s intervals before and 1 s following illumination; samples were partially dehydrated. In the spectrum obtained, a spectral feature at 1512 cm^{-1} was altered in intensity upon $^{13}C_1$ tyrosine labeling but not upon $^{13}C_6$ tyrosine labeling (*47*). There are several possible explanations for the failure to observe the 1478 cm^{-1} line of Z• under these alternate conditions. First, because Z• normally decays on the millisecond time scale in the PSII preparation employed (for example, see refs *17* and *48*), data were acquired in a time regime where the vibrational contributions of Z• may not be

detectable. Second, the high ionic strength buffer employed would be expected, from the results reported here, to change PSII structure and may lead to frequency shifts in the $Z^{\bullet} - Z$ spectrum. Third, the buffer itself may be contributing to the spectrum. These three explanations are not mutually exclusive. Negative control experiments would be helpful in distinguishing among these possibilities (*17*).

Difference infrared spectroscopy has the potential to give new insight into structure/function relationships in photosystem II. These experiments have been aimed at a clarification of vibrational assignments. Our work shows that the failure to observe the 1477 cm^{-1} line of $D^{\bullet}$, under an unusual set of sample conditions, is due to the biochemical conditions employed. These data support our previous assignments of spectral features to redox-active tyrosines in photosystem II (*11*, *14*−*18*).

ACKNOWLEDGMENT

We gratefully acknowledge Dr. Albert Markhart III and his group for allowing us the extended use of their fluorometer. Ms. E. T. Gonzalez is acknowledged for her initial work on this project. We also thank Mr. A. Ouellette and Dr. L. A. Anderson, who prepared some of the spinach photosystem II samples employed in this study.

REFERENCES

1. Barry, B. A., Boerner, R. J., and de Paula, J. C. (1994) in *The Molecular Biology of the Cyanobacteria* (Bryant, D., Ed.) pp 215−257, Kluwer Academic Publishers, Dordrecht.
2. Britt, R. D. (1996) in *Oxygenic Photosynthesis: The Light Reactions* (Ort, D. R., and Yocum, C. F., Eds.) pp 137−164, Kluwer Academic Publisher, Dordrecht.
3. Barry, B. A., and Babcock, G. T. (1987) *Proc. Natl. Acad. Sci. U.S.A. 84*, 7099−7103.
4. Debus, R. J., Barry, B. A., Babcock, G. T., and McIntosh, L. (1988) *Proc. Natl. Acad. Sci. U.S.A. 85*, 427−430.
5. Vermaas, W. F. J., Rutherford, A. W., and Hansson, O. (1988) *Proc. Natl. Acad. Sci. U.S.A. 85*, 8477−8481.
6. Vass, I., and Styring, S. (1991) *Biochemistry 30*, 830−839.
7. Buser, C. A., Thompson, L. K., Diner, B. A., and Brudvig, G. W. (1990) *Biochemistry 29*, 8977−8985.
8. Braiman, M. S., and Rothschild, K. J. (1988) *Annu. Rev. Biophys. Biophys. Chem. 17*, 541−570.
9. Noguchi, T., Ono, T.-a., and Inoue, Y. (1995) *Biochim. Biophys. Acta 1232*, 59−66.
10. Hienerwadel, R., Boussac, A., Breton, J., Diner, B. A., and Berthomieu, C. (1997) *Biochemistry 36*, 14712−14723.
11. Kim, S., Liang, J., and Barry, B. A. (1997) *Proc. Natl. Acad. Sci. U.S.A. 94*, 14406−14411.
12. Steenhuis, J. J., and Barry, B. A. (1997) *J. Phys. Chem. B 101*, 6652−6660.
13. Zhang, H., Razeghifard, M. R., Fischer, G., and Wydrzynski, T. (1997) *Biochemistry 36*, 11762−11768.
14. MacDonald, G. M., and Barry, B. A. (1992) *Biochemistry 31*, 9848−9856.
15. MacDonald, G. M., Bixby, K. A., and Barry, B. A. (1993) *Proc. Natl. Acad. Sci. U.S.A. 90*, 11024−11028.
16. Bernard, M. T., MacDonald, G. M., Nguyen, A. P., Debus, R. J., and Barry, B. A. (1995) *J. Biol. Chem. 270*, 1589−1594.
17. Kim, S., Ayala, I., Steenhuis, S., Gonzalez, E. T., Razeghifard, M. R., and Barry, B. A. (1998) *Biochim. Biophys. Acta 1364*, 337−360; publisher's correction, *Biochim. Biophys. Acta 1366*, 330−354.
18. Kim, S., and Barry, B. A. (1998) *Biophys. J. 74*, 2588−2600.
19. Hienerwadel, R., Boussac, A., Breton, J., and Berthomieu, C. (1996) *Biochemistry 35*, 15447−15460.
20. Patzlaff, J. S., and Barry, B. A. (1996) *Biochemistry 35*, 7802−7811.
21. Berthold, D. A., Babcock, G. T., and Yocum, C. F. (1981) FEBS Lett. 134, 231−234.
22. Lichtenthaler, H. K. (1987) *Methods Enzymol. 148*, 350−382.
23. Barry, B. A. (1995) *Methods Enzymol. 258*, 303−319.
24. Boerner, R. J., Nguyen, A. P., Barry, B. A., and Debus, R. J. (1992) *Biochemistry 31*, 6660−6672.
25. Metz, J. G., Pakrasi, H. B., Seibert, M., and Arntzen, C. J. (1986) *FEBS Lett. 205*, 269−274.
26. Griffith, W. P., and Turner, G. T. (1970) *J. Chem. Soc. A*, 858−861.
27. Cotton, F. A., and Wilkinson, G. (1988) *Advanced Inorganic Chemistry*, pp 713−720, John Wiley & Sons, New York.
28. Krimm, S., and Bandekar, J. (1986) in *Advances in Protein Chemistry* (Anfinsen, C. B., Edsall, J. T., and Richards, F. M., Eds.) pp 181−364, Academic Press, New York.
29. Byler, D. M., and Susi, H. (1986) *Biopolymers 25*, 469−487.
30. Susi, H., and Byler, D. M. (1986) *Methods Enzymol. 130*, 290−311.
31. Surewicz, W. K., Mantsch, H. A., and Chapman, D. (1993) *Biochemistry 32*, 389−394.
32. Rivas, J. D. L., and Barber, J. (1997) *Biochemistry 36*, 8897−8903.
33. Huang, D. B., Ainsworth, C. F., Stevens, F. J., and Schiffer, M. (1996) *Proc. Natl. Acad. Sci. U.S.A. 93*, 7017−7021.
34. Tripathi, G. N. R., and Schuler, R. H. (1984) *J. Chem. Phys. 81*, 113−121.
35. Johnson, C. R., Ludwig, M., and Asher, S. A. (1986) *J. Am. Chem. Soc. 108*, 905−912.
36. Berthomieu, C., Boussac, A., Mantele, W., Breton, J., and Nabedryk, E. (1992) *Biochemistry 31*, 11460−11471.
37. MacDonald, G. M., Steenhuis, J. J., and Barry, B. A. (1995) *J. Biol. Chem. 270*, 8420−8428.
38. Steenhuis, J. J., and Barry, B. A. (1998) *J. Phys. Chem. B 102*, 4−8.
39. He, W.-Z., Newell, W. R., Haris, P. I., Chapman, D., and Barber, J. (1991) *Biochemistry 30*, 4552−4559.
40. Zhang, H., Yamamoto, Y., Ishikawa, Y., Zhang, W., Fischer, G., and Wydrzynski, T. (1997) *Photosynth. Res. 52*, 215−223.
41. Clark, A. H., Saunderson, D. H., and Suggett, A. (1981) *Int. J. Pept. Protein Res. 17*, 353−364.
42. Copley, R. R., and Barton, G. J. (1994) *J. Mol. Biol. 242*, 321−329.
43. van der Spoel, D., Feenstra, K. A., Hemminga, M. A., and Berendsen, H. J. C. (1996) *Biophys. J. 71*, 2920−2932.
44. Gopher, A., Blatt, Y., Schonfeld, M., Okamura, M. Y., Feher, G., and Montal, M. (1985) *Biophys. J. 48*, 311−320.
45. Pimental, G. C., and McClellan, A. L. (1960) *The hydrogen bond*, pp 67−141, W. H. Freeman and Company, San Francisco.
46. Barry, B. A. (1993) *Photochem. Photobio. 57*, 179−188.
47. Berthomieu, C., Hienerwadel, R., Boussac, A., Breton, J., and Diner, B. A. (1998) *Biochemistry*, 10547−10554.
48. Metz, J. G., Nixon, P. J., Rogner, M., Brudvig, G. W., and Diner, B. A. (1989) *Biochemistry 28*, 6960−6969.

BI981318V